

# Local Quantum Gravity

N. Christiansen,<sup>1</sup> B. Knorr,<sup>2</sup> J. Meibohm,<sup>1</sup> J. M. Pawłowski,<sup>1,3</sup> and M. Reichert<sup>1</sup>

<sup>1</sup>*Institut für Theoretische Physik, Universität Heidelberg, Philosophenweg 16, 69120 Heidelberg, Germany*

<sup>2</sup>*Theoretisch-Physikalisches Institut, Universität Jena, Max-Wien-Platz 1, 07743 Jena, Germany*

<sup>3</sup>*ExtreMe Matter Institute EMMI, GSI Helmholtzzentrum für Schwerionenforschung mbH, Planckstr. 1, 64291 Darmstadt, Germany*

We investigate the ultraviolet behaviour of quantum gravity within a functional renormalisation group approach. The present setup includes the full ghost and graviton propagators and, for the first time, the dynamical graviton three-point function. The latter gives access to the coupling of dynamical gravitons and makes the system minimally self-consistent. The resulting phase diagram confirms the asymptotic safety scenario in quantum gravity with a non-trivial UV fixed point.

A well-defined Wilsonian block spinning requires locality of the flow in momentum space. This property is discussed in the context of functional renormalisation group flows. We show that momentum locality of graviton correlation functions is non-trivially linked to diffeomorphism invariance, and is realised in the present setup.

*Introduction* - One of the major challenges in theoretical physics is the unification of the standard model of particle physics with gravity. A very promising route is the asymptotic safety scenario proposed by Weinberg in 1976 [1]. In this scenario, quantum gravity exhibits a nontrivial ultraviolet (UV) fixed point with a finite dimensional critical hypersurface, which renders the theory finite and predictive even beyond the Planck scale.

A large amount of work in the recent years supports the existence of such a gravitational UV fixed point. A non-perturbative method of choice for studying the asymptotic safety scenario is the functional renormalisation group. The simplest approximation in this approach is given by an RG-improved Einstein-Hilbert truncation. In the latter, one retains only two couplings, namely Newton's coupling  $G_N$  and the cosmological constant  $\Lambda$  [2]. Already this basic truncation exhibits a UV fixed point, and truncations beyond Einstein-Hilbert, e.g. [3–9], provide further evidence for its existence. The implementation of diffeomorphism invariance and the related interplay of background and fluctuation fields is addressed in e.g. [3–5, 10, 11]. The analysis of the infrared (IR) limit is subject to the studies [3–5, 12]. The first smooth, classical IR limit was found in [4], delivering a global picture of quantum gravity.

In this letter we present the first calculation of a genuine dynamical gravitational coupling. Here we build on the general setup for flows of fully momentum dependent vertex functions in quantum gravity developed in [3, 4]. This expansion naturally resolves the physically important difference between the graviton wave-function renormalisation and the gravitational couplings. The existence of the UV and IR fixed points is confirmed in this enhanced approximation, thus providing further evidence for the asymptotic safety scenario. Interestingly, the ultraviolet fixed point exhibits one irrelevant direction, along with two relevant ones, in accordance with the hypothesis of a finite dimensional critical hypersurface. For related results in  $f(R)$  gravity see e.g. [6, 13].

A well-defined Wilsonian block spinning requires locality of the flow in momentum space. Here we show

that the flows of the graviton two- and three-point functions are local in momentum space. This non-trivial property is linked to diffeomorphism invariance.

*The Functional Renormalisation Group* - The present computation of correlation functions in quantum gravity is based on the functional renormalisation group approach to gravity [2]. In this framework momenta smaller than the infrared cutoff scale  $k$  are suppressed by including a momentum dependent mass function  $R_k$ . This leads to a scale-dependent effective action  $\Gamma_k[\bar{g}, \phi]$ . The full metric  $g = \bar{g} + h$  is expanded around a fixed background metric  $\bar{g}$ , and the fluctuation super-field  $\phi = (h, c, \bar{c})$  comprises the graviton fluctuations  $h$  and the (anti-) ghost fields  $c, \bar{c}$ . The scale-dependence of the effective action is governed by the flow of  $\Gamma_k$ , to wit

$$\dot{\Gamma}_k = \frac{1}{2} \text{Tr} \left[ \frac{1}{\Gamma_k^{(2)} + R_k} \dot{R}_k \right]_{hh} - \text{Tr} \left[ \frac{1}{\Gamma_k^{(2)} + R_k} \dot{R}_k \right]_{\bar{c}c}. \quad (1)$$

In (1) we have introduced the notation  $\dot{f} = \partial_t f$  for  $t = \log k/k_{\text{in}}$ -derivatives with some reference scale  $k_{\text{in}}$ , usually taken to be the initial scale. The trace implies integrals over continuous and sums over discrete indices, and  $\Gamma_k^{(2)}$  is the second derivative of the effective action with respect to the fluctuation fields.

An important issue in quantum gravity is the background independence of physical observables. We emphasise that in the present framework, based on an effective action  $\Gamma[\bar{g}, \phi]$ , we have the paradoxical situation that the background independence of observables necessitates the background dependence of the vertex functions  $\Gamma^{(n)}$  of the dynamical fields. Importantly, an ansatz  $\Gamma[\bar{g}, \phi] = \Gamma[\bar{g} + \phi]$  violates background independence and dynamical diffeomorphism invariance, see e.g. [5, 14, 15].

A setup that disentangles the dependence on  $\bar{g}$  and  $\phi$  in terms of a vertex expansion has been constructed in [3, 4]. In this vein, a vertex expansion about a flat Euclidean background is used in this work to self-consistently determine the flow of the couplings from the two- and three-point functions.

*Locality* - The functional renormalisation group is based on the idea of a successive integration of momentum shells, or, more generally, spectral shells of spectral values of the given kinetic operator. Hence, it relies on the distinction of small and large momentum or spectral modes. A functional RG step implements the physics of momentum/spectral modes at a given scale  $k$  and is inherently related to local interactions.

Locality in momentum space implies in particular that the flows of vertices at a given momentum scale  $k$  decay relative to the vertex itself if all momentum transfers (momentum channels)  $t_i$  are taken to infinity. For example, for the four-point vertex we have  $t_1, t_2, t_3$  being the well-known  $s, t, u$ -channels, with e.g.  $s = (p_1 + p_2)^2$ . Hence, locality reads schematically

$$\lim_{t_i/k^2 \rightarrow \infty} \frac{|\dot{\Gamma}_k^{(n)}(\mathbf{p})|}{|\Gamma_k^{(n)}(\mathbf{p})|} = 0, \quad \text{with } \mathbf{p} = (p_1, \dots, p_n), \quad (2)$$

where a projection on one of the tensor structure of the vertex is implied. For the limit (2) each diagram in the flow of a given vertex has an infinite momentum transfer. Thus, the diagrams are only sensitive to fluctuations far above the cutoff scale.

It is easily proven that (2) applies to standard renormalisable quantum field theories in four dimensions including non-Abelian gauge theories that involve momentum-dependent couplings. In these theories, the locality property follows from power-counting arguments. However, for perturbatively non-renormalisable theories in four dimensions power counting suggests non-local flows and (2) must be a consequence of non-trivial cancellations. In gravity this has been shown for the graviton propagator [3, 4]. It is also reflected in the symmetry relation between graviton diagrams contributing to the Yang-Mills propagator [16]. Moreover, it is easily verified that a  $\phi^4$ -theory with a momentum-dependent coupling such as  $\int_x \phi^2 \partial^2 \phi^2$  does not satisfy the locality condition (2), as no cancellation between tensor structures is possible. This entails that momentum locality in quantum gravity is linked to diffeomorphism invariance, and we conjecture that it is indeed rooted in the latter.

Note that (2) does not hold, even for quantum field theories which are perturbatively renormalisable in four dimensions, if some of the channels  $t_i/k^2$  stay finite: the flow always involves diagrams with a finite momentum transfer. However, those diagrams correspond to IR processes such as Bremsstrahlung, which is why they do not reflect the UV behaviour of the theory. In summary the above discussion suggests that the relation (2) is a necessary requirement for local quantum field theories.

In this work, we show (see page 3 & 4) that (2) also applies to the graviton three-point function. Together with the momentum locality of the two-point function shown in [3, 4] this provides strong indications for the momentum locality of RG-gravity. Figure 1 depicts the momentum dependence of the flows for the graviton two-

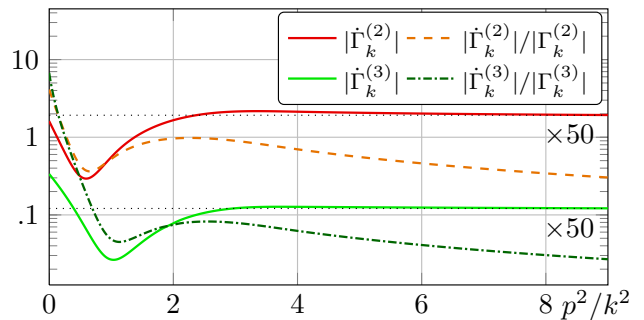


FIG. 1. Logarithmic plot of the flows  $|\dot{\Gamma}_k^{(2)}|$  and  $|\dot{\Gamma}_k^{(3)}|$  (solid red and light green curves) and the corresponding ratios  $|\dot{\Gamma}_k^{(2)}|/|\Gamma_k^{(2)}|$  and  $|\dot{\Gamma}_k^{(3)}|/|\Gamma_k^{(3)}|$  (dashed orange and dash-dotted dark green curves) as functions of  $p^2/k^2$ . The norm refers to the tensor projection discussed below (6). All quantities are evaluated at  $(g, \mu_h, \lambda_3) = (1, 0.1, -0.7)$ . The flows are multiplied with 50 for convenience. The ratios decay with  $1/p^2$  for large  $p$  since the associated flows quickly approach constant values, satisfying (2).

and three-point functions,  $|\dot{\Gamma}_k^{(2)}|$  and  $|\dot{\Gamma}_k^{(3)}|$ , respectively as well as the corresponding ratios according to (2). Since  $|\dot{\Gamma}_k^{(2)}|$  and  $|\dot{\Gamma}_k^{(3)}|$  quickly approach constants, the ratios decay with  $1/p^2$  for large momenta.

*Flows of Correlation Functions* - The flow of the three-point function is obtained by three field derivatives of the flow equation for the effective action (1). It is depicted in Figure 2. We build on the parametrisation for vertex functions introduced in [4, 17]. Our ansatz is given by

$$\Gamma_k^{(\phi_1 \dots \phi_n)}(\mathbf{p}) = \left( \prod_{i=1}^n \sqrt{Z_{\phi_i}(p_i^2)} \right) G_n^{\frac{n}{2}-1} \mathcal{T}^{(n)}(\mathbf{p}; \Lambda_n). \quad (3)$$

where  $\mathcal{T}^{(n)}$  is the classical tensor structure of the vertex to be specified in (4). Other tensor structures are neglected. Moreover,  $Z_{\phi_i}(p_i^2)$  denotes the wave function renormalisation corresponding to the field  $\phi_i(p_i)$  and captures the renormalisation group running of the vertex. The coupling  $G_n(\mathbf{p})$  represents the gravitational vertex coupling of  $n$ -th order, and  $\Lambda_n$  parametrises the momentum independent part of  $\Gamma_k^{(n)}$ . Note that  $G_3$  is the first dynamical gravitational coupling and its flow is extracted from the graviton three-point function. In this work we approximate all  $G_n$  as one, momentum-independent coupling,  $G_n(\mathbf{p}) = G_3$ . We shall show that the momentum-dependence of the vertex is already captured well with that of the factors  $Z_{\phi_i}^{1/2}(p_i^2)$ . We also emphasise that  $G_n$ ,  $\Lambda_n$  and  $Z_{\phi_i}$  are scale dependent, although the subscript  $k$  is suppressed here and in the following.

Finally, the tensor structures  $\mathcal{T}^{(n)}$  are obtained from the classical gauge fixed Einstein-Hilbert action,

$$\mathcal{T}^{(n)}(\mathbf{p}; \Lambda_n) = G_N S^{(n)}(\mathbf{p}; \Lambda \rightarrow \Lambda_n), \quad (4)$$

and

$$S = \frac{1}{16\pi G_N} \int d^4x \sqrt{g} (2\Lambda - R) + S_{\text{gf}} + S_{\text{gh}}. \quad (5)$$

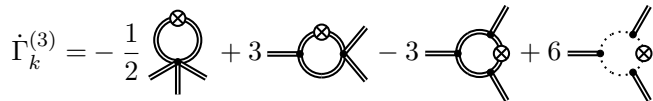


FIG. 2. Diagrammatic representation of the flow of the three-graviton vertex. Double and dashed lines represent graviton and ghost propagators respectively, filled circles denote dressed vertices. Crossed circles are regulator insertions. All diagrams are symmetrised with respect to the interchange of external momenta  $\mathbf{p}$ .

In (5),  $R$  is the Ricci scalar and  $\Lambda$  the cosmological constant. The terms  $S_{\text{gh}}$  and  $S_{\text{gf}}$  are the usual Faddeev-Popov ghost action and the gauge fixing term, respectively. We employ a De-Donder-type linear gauge condition in the Landau limit of vanishing gauge parameter.

The right hand side of the vertex flows usually includes all types of tensor structures admitted by symmetry irrespective of the ansatz for the vertices. For the flow equations for the couplings  $\Lambda_n$  and  $G_n$  we have to project the tensorial vertex flow appropriately: we focus on the transverse-traceless parts of the flow, and reduce all external graviton legs to its spin-2 parts by using transverse-traceless projectors  $\Pi_{\text{TT}}$ . The flow of  $\Lambda_n$  in (4) is extracted from the momentum independent part of the  $n$ -th vertex flow at  $\mathbf{p} = 0$ . Consequently, we decompose  $\mathcal{T}^{(n)}(\mathbf{p}, \Lambda_n)$  into its momentum independent part  $\mathcal{T}^{(n)}(0, 1)$  and the part  $\mathcal{T}^{(n)}(\mathbf{p}, 0)$ , which is quadratic in  $\mathbf{p}$ , according to

$$\mathcal{T}^{(n)}(\mathbf{p}; \Lambda_n) = \Lambda_n \mathcal{T}^{(n)}(0; 1) + \mathcal{T}^{(n)}(\mathbf{p}; 0). \quad (6)$$

The full tensor flow with transverse-traceless external legs is then contracted with  $\mathcal{T}^{(n)}(0; 1)$  or  $\mathcal{T}^{(n)}(\mathbf{p}; 0)$  in order to yield scalar expressions that are related to the flow of  $\Lambda_n$  or  $G_n$ , respectively. In particular, we denote the contraction of the RHS with  $\mathcal{T}^{(n)}(0, 1)$  and  $\mathcal{T}^{(n)}(\mathbf{p}, 0)/\mathbf{p}^2$  by  $\text{Flow}_{\Lambda}^{(n)}$  and  $\text{Flow}_G^{(n)}$ , respectively. The factor of  $1/\mathbf{p}^2$  in the definition of the flow for the gravitational coupling accounts for the fact that the corresponding tensor projector is proportional to  $p^2$ . For convenience, the definition of  $\text{Flow}^{(n)}$  also includes the factor  $\prod_i Z_h^{-1/2}(p_i)$ . For the graviton three-point function these objects take the generic form

$$\text{Flow}_{\Lambda/G}^{(3)} = \int_q (\dot{r}(q) - \eta_{\phi_i}(q^2)r(q)) F_{\phi_i, \Lambda/G}(\mathbf{p}, q, G_n, \Lambda_n), \quad (7)$$

where  $n \in \{3, 4, 5\}$  and a sum over species of fields  $\phi_i$  is understood. Furthermore,  $r$  is the shape function of the regulator. The contributions encoded in  $F_{\phi_i}$  originate from the diagrams displayed in Figure 2. Note that (7) is only a function of the anomalous dimension

$$\eta_{\phi_i}(p^2) := -\dot{Z}_{\phi_i}(p^2)/Z_{\phi_i}(p^2), \quad (8)$$

since all wave function renormalisations  $Z_{\phi_i}$  drop out. The expressions for the flow of the three-point function

still depend on the external momenta  $\mathbf{p} = (p_1, p_2, p_3)$ , where  $p_3$  can be eliminated using momentum conservation. Therefore, the kinematic degrees of freedom can be parametrised by the absolute values of the remaining two momenta  $|p_1|$ ,  $|p_2|$  and the angle  $\vartheta_{12}$  between them. For the proof of locality we work with the most general momentum configuration. For the flows  $\text{Flow}_{\Lambda/G}^{(3)}$  the maximally symmetric momentum configuration is used,

$$p := |p_1| = |p_2| \quad \vartheta_{12} = 2\pi/3. \quad (9)$$

In summary, we have specified a projection procedure for the spacetime indices and a kinematic configuration for the graviton field momenta. It remains to relate  $\text{Flow}_G^{(3)}$  and  $\text{Flow}_{\Lambda}^{(3)}$  to the flow of the couplings  $G_3$  and  $\Lambda_3$ , respectively. The flow of  $G_3$  is most conveniently isolated by evaluating the projected flow at two momentum scales  $p = k$  and  $p = 0$  and subtracting the results. For the dimensionless coupling  $g_3 = k^2 G_3$  we obtain

$$\dot{g}_3 = (2 + 3\eta_h(k^2))g_3 - \frac{24}{19}(\eta_h(k^2) - \eta_h(0))\lambda_3 g_3 + 2\mathcal{N}_g \sqrt{g_3} k \left( \text{Flow}_G^{(3)}(k^2) - \text{Flow}_G^{(3)}(0) \right), \quad (10)$$

with a normalisation factor  $\mathcal{N}_g^{-1} := \mathcal{T}^{(3)}(k; 0) \circ \Pi_{\text{TT}}^3 \circ \mathcal{T}^{(3)}(k; 0)$ , where  $\circ$  denotes the pairwise contraction of indices. Another possibility is the evaluation with a  $p^2$ -derivative at  $p = 0$ . This procedure is less accurate in approximating the momentum dependence of the flow. On the other hand, it allows for an analytic flow equation for the couplings  $G_3$ . The difference between these momentum projections is discussed below. The flow of the dimensionless coupling  $\lambda_3 = \Lambda_3/k^2$  is obtained by evaluating the flow at  $p = 0$ , which leads to

$$\dot{\lambda}_3 = \left( \frac{3}{2}\eta_h(0) - 1 - \frac{\dot{g}_3}{2g_3} \right) \lambda_3 + \frac{\mathcal{N}_{\lambda}}{\sqrt{g_3}} \text{Flow}_{\Lambda}^{(3)}(0), \quad (11)$$

with  $\mathcal{N}_{\lambda}^{-1} := \mathcal{T}^{(3)}(0; 1) \circ \Pi_{\text{TT}}^3 \circ \mathcal{T}^{(3)}(0; 1)$ . The setup is complemented by flow equations for the graviton mass parameter  $\mu = -2\Lambda_2/k^2$ , the fully momentum dependent anomalous dimensions  $\eta_{\phi_i}(p^2)$  and the coupling of the one-point function  $\lambda_1/\sqrt{g_1} = \Lambda_1 G_1^{-1/2}/k^3$ . The flows for the couplings  $\mu$  and  $\lambda_1/\sqrt{g_1}$  are extracted from the graviton two- and one-point functions at vanishing external momenta, respectively. The anomalous dimensions  $\eta_{\phi_i}(p^2)$  are solutions to Fredholm integral equations, extracted from the two-point functions, see [4].

*Proof of Locality* - In order to prove (2) for the three point function, an arbitrary kinematic configuration is used and parametrised by  $|p_1|$ ,  $|p_2|$  and the angle  $\vartheta_{12}$ . The large momentum limit is then characterised by  $|p_1| = |p_2| = p \rightarrow \infty$ . Simple power counting of the momentum structure of the flow leads to the naïve expectation that  $\lim_{p/k \rightarrow \infty} \text{Flow}_G^{(3)} \sim p^2$ . In this case the ratio in (2) would tend to a constant. However, an analytic asymptotic expansion around  $p = \infty$  shows

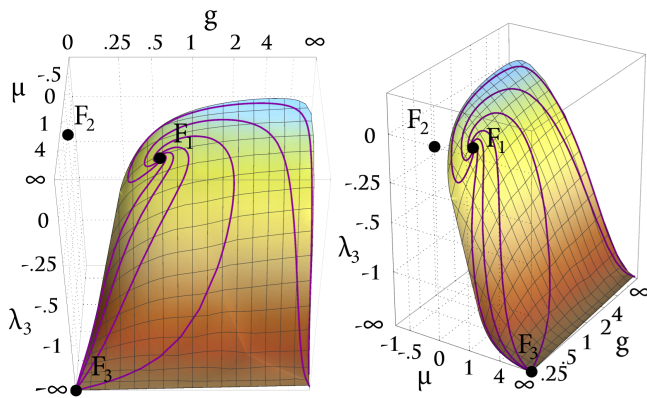


FIG. 3. Phase diagram for the couplings  $g$ ,  $\lambda_3$  and  $\mu$  in two different views. The phase diagram was calculated using the analytic equations (14). The system exhibits a non-trivial UV fixed point,  $F_1$ , with two attractive and one repulsive direction. The Gaussian fixed point and a non-trivial IR fixed point are denoted as  $F_2$  and  $F_3$ , respectively. The set of trajectories that approach  $F_1$  constitutes two-dimensional UV critical hypersurface represented in gradient colours.

that the  $p^2$ -contribution vanishes identically in the large-momentum limit by non-trivial cancellations between all diagrams in Figure 2. As a consequence,  $\lim_{p/k \rightarrow \infty} \text{Flow}_G^{(3)}$  tends to a constant and the ratio in (2) vanishes. This is valid for all values of the angle  $\vartheta_{12}$ , i.e. for all kinematic configurations. For an explicit example see Figure 1 for the symmetric momentum configuration. Figure 1 further displays that (2) is also satisfied by the graviton two-point function, see also [3, 4]. We conclude that locality is always satisfied by the flows of two- and three-point functions. We emphasise again that it is indispensable that all external momenta are taken to infinity. Indeed, for configurations with mixed UV-IR limit equation (2) does not hold.

*UV Fixed Point* - Fixed points are defined by vanishing flows of all dimensionless dynamical couplings, that is  $g_3$ ,  $\lambda_3$  and  $\mu$  in the present setup. Most importantly, we find a UV fixed point with one irrelevant direction that is approximately directed along the  $\lambda_3$ -axis.

The following results are obtained with the regulator  $R_\phi(x) = \Gamma_k^{(\phi\phi)}|_{\mu=0}(x)r(x)$  where  $xr(x) = (1-x)\theta(1-x)$ . Moreover, we identify  $\lambda_3 \equiv \lambda_4 \equiv \lambda_5$  in order to close the flow equations, and use the notation  $g := g_3$ . The UV fixed point described below is obtained with the finite difference procedure, leading to the flow equations (10) and (11), as well as the one for  $\mu$  already presented in [4]. The anomalous dimensions are evaluated with their full momentum dependence. The fixed point values read

$$(g^*, \mu^*, \lambda_3^*) = (0.66, -0.59, 0.11), \quad (12)$$

with the critical exponents  $\theta_1$ ,  $\theta_2$  and  $\theta_3$  given by

$$(\theta_{1/2}, \theta_3) = (-1.4 \pm 4.1i, 14). \quad (13)$$

TABLE I. Properties of the UV fixed point for different momentum parametrisations, namely using a finite difference of the flow and a derivative at  $p = 0$ . The values acquired with the latter correspond to the analytic equations given in (14). Note, that  $\lambda_1/\sqrt{g_1}$  is a non-dynamical background coupling originating from the graviton one-point function.

	Finite difference		Derivative	
	$\eta_{\phi_i}(p^2)$	$\eta_{\phi_i} = 0$	$\eta_{\phi_i}(p^2)$	$\eta_{\phi_i} = 0$
$g^*$	0.66	0.96	0.58	0.57
$\mu_h^*$	-0.59	-0.35	-0.44	-0.16
$\lambda_3^*$	0.11	-0.024	0.028	-0.16
$\lambda_1^*/\sqrt{g_1^*}$	0.39	0.19	0.22	0.11
EVs	$-1.4 \pm 4.1i$	$-2.1 \pm 2.4i$	$-1.6 \pm 5.5$	$-1.5 \pm 1.8i$
	14	5.8	6.5	1.6
	-2.2	-3	-2.5	-3

As already mentioned above, the UV fixed point (12) has the interesting property that it is not fully UV attractive: it exhibits two relevant and one irrelevant direction. In (13), this is reflected by two critical exponents with negative real parts,  $\theta_1$  and  $\theta_2$ , and one with positive real part,  $\theta_3$ . The irrelevant direction of the UV fixed point (12) is approximately directed along the  $\lambda_3$  axis. The critical exponents corresponding to the UV relevant directions of the fixed points are complex, which accounts for a spiral behaviour of RG-trajectories in the vicinity of the UV fixed point. Note, that  $\theta_3$  in (13) is one order of magnitude larger than  $\theta_1$  and  $\theta_2$ . This kind of instability of critical exponents was also found in [6] within  $f(R)$ -gravity. There, a convergence of the critical exponents to smaller values was observed after the inclusion of higher order operators, i.e. higher powers  $R^n$ . Similarly, we expect  $\theta_3$  to become smaller, if dynamical couplings  $g_4$  and  $\lambda_4$  are included. Finally, we have checked numerically that the momentum dependencies of our ansatz for the vertex dressing and that of  $\text{Flow}^{(2)}$  and  $\text{Flow}_G^{(3)}$  are in very good agreement. Therefore, a momentum independent  $G_3$  is a valid approximation over the whole momentum range. In particular, the full momentum dependence of the anomalous dimensions was found to model very accurately the higher order  $p$ -dependence of  $\text{Flow}_G^{(3)}$ .

*Global Phase Diagram and Analytic Flow Equations* - The flow equation (10) does not have a closed analytic form. However, for a more accessible presentation, analytic flow equations are favourable. An analytic expression for  $\dot{g}$  is obtained by taking a derivative of  $\text{Flow}_G^{(3)}$  with respect to  $p^2$  at  $p = 0$ . We stress, that this method is considerably less accurate in modelling the momentum dependence of the flow. Nonetheless, the resulting analytic flow equation for  $g$  shares the main features with (10). This even holds for all anomalous dimensions set to zero,  $\eta_{\phi_i} = 0$ . Table I displays the properties of the non-trivial fixed point as obtained from the different methods.

The analytic flow equations for the presented vertex

flow of gravity with  $\eta_{\phi_i} = 0$  are given by

$$\begin{aligned} \dot{g} &= 2g + \frac{8g^2}{19\pi} \left( \frac{584\lambda_3^3 - 910\lambda_3^2 + 445\lambda_3 - \frac{299}{4}}{15(\mu+1)^5} - \frac{47}{8(\mu+1)^2} \right. \\ &\quad \left. - \frac{5}{8} + \frac{864\lambda_3^3 + 133\lambda_3^2 - 112\lambda_3 + \frac{49}{4}}{6(\mu+1)^4} - \frac{60\lambda_3^2 - 58\lambda_3 - 15}{6(\mu+1)^3} \right), \\ \dot{\lambda}_3 &= - \left( 1 + \frac{\dot{g}}{2g} \right) \lambda_3 + \frac{g}{\pi} \left( \frac{2\lambda_3^3 - 4\lambda_3^2 + 3\lambda_3 - \frac{11}{20}}{(\mu+1)^4} \right. \\ &\quad \left. - 4 \frac{4\lambda_3^2 - \lambda_3}{(\mu+1)^3} + \frac{1 - 3\lambda_3}{(\mu+1)^2} + \frac{6}{5} \right), \\ \dot{\mu} &= -2\mu + \frac{2g}{\pi} \left( \frac{16\lambda_3^2 - 8\lambda_3 + \frac{7}{4}}{3(\mu+1)^3} + \frac{2\lambda_3 - 1}{(\mu+1)^2} - 1 \right), \\ \partial_t \left( \frac{\lambda_1}{\sqrt{g_1}} \right) &= -3 \frac{\lambda_1}{\sqrt{g_1}} + \frac{\sqrt{g}}{2\pi} \left( \frac{1}{(\mu+1)^2} + \frac{4}{3} \right). \end{aligned} \quad (14)$$

Figure 3 shows the phase diagram for the couplings  $(g, \mu, \lambda_3)$  as calculated from (14). The purple lines are trajectories along the flow that terminate at the non-trivial UV fixed point  $F_1$ . The set of all trajectories constitutes the two-dimensional critical hypersurface represented in gradient colours. In the IR, the trajectories flow towards  $F_3 = (0, \infty, -\infty)$  or, alternatively, towards  $(\infty, \infty, -\infty)$ . The IR fixed point  $F_3$  was also observed in [4]. In the vicinity of  $F_3$  all couplings scale classically since for  $\mu \rightarrow \infty$  the loop contributions to the flow tend to zero. Neither the trivial Gaussian fixed point  $F_2$ , nor the third, non-trivial IR fixed point, which was first found in [4] and is located at  $(0, -1, \infty)$ , are reached by any UV-finite trajectory in the presented setup. For the latter, this is expected to change if the vertices are expanded about a non-flat background [18].

A detailed IR analysis is beyond the scope of this letter and is postponed to future work.

*Summary* - We have presented the first genuine calculation of dynamical gravitational couplings based on a vertex flow. The dynamical parameters are the graviton-mass parameter  $\mu$ , the Newton coupling  $g$  derived from the graviton three-point function, and the coupling  $\lambda_3$  of its momentum-independent part. The full momentum-dependence of the propagators is encoded in  $\eta_h(p^2)$  and  $\eta_c(p^2)$ . The flows of these quantities constitute a minimally self-consistent truncation of the system of dynamical couplings in quantum gravity. In the UV we find a fixed point with two relevant and one irrelevant direction, the latter being approximately directed along the  $\lambda_3$ -axis. This hints at a finite dimensional critical UV-surface, and supports the asymptotic safety scenario.

We have introduced the property of momentum locality for vertex flows. It is suggestive that this property is a necessary requirement for local quantum field theories. We have shown that it is non-trivially realised for the graviton two- and three-point functions, being linked to diffeomorphism invariance.

Currently, we extend the present work to improved approximations including higher order correlation functions and non-trivial backgrounds. This allows to evaluate the convergence of the present expansion scheme and its dependence on the expansion point. Non-trivial backgrounds are expected to play an important rôle for the fate of the IR fixed point at  $\mu = -1$ . Higher order vertices give further insights into the important feature of momentum locality.

**Acknowledgements** We thank A. Eichhorn, K. Falls, H. Gies, A. Rodigast and C. Wetterich for discussions. NC acknowledges funding from the HGSFP, MR from IMPRS-PTFS, and BK from GRK 1523/2, and Wi 777/11-1. This work is supported by the Helmholtz Alliance HA216/EMMI and by ERC-AdG-290623.

- 
- [1] S. Weinberg, General Relativity: An Einstein centenary survey, Eds. Hawking, S.W., Israel, W; Cambridge University Press, 790 (1979).
- [2] M. Reuter, *Phys. Rev.* **D57**, 971 (1998), [arXiv:hep-th/9605030](#).
- [3] N. Christiansen, D. F. Litim, J. M. Pawłowski, and A. Rodigast, *Phys.Lett.* **B728**, 114 (2014), [arXiv:1209.4038 \[hep-th\]](#).
- [4] N. Christiansen, B. Knorr, J. M. Pawłowski, and A. Rodigast, (2014), [arXiv:1403.1232 \[hep-th\]](#).
- [5] I. Donkin and J. M. Pawłowski, (2012), [arXiv:1203.4207 \[hep-th\]](#).
- [6] K. Falls, D. F. Litim, K. Nikolakopoulos, and C. Rahmede, (2014), [arXiv:1410.4815 \[hep-th\]](#).
- [7] A. Codello, R. Percacci, and C. Rahmede, *Int. J. Mod. Phys.* **A23**, 143 (2008), [arXiv:0705.1769 \[hep-th\]](#).
- [8] P. F. Machado and F. Saueressig, *Phys. Rev.* **D77**, 124045 (2008), [arXiv:0712.0445 \[hep-th\]](#).
- [9] D. Benedetti, P. F. Machado, and F. Saueressig, *Mod. Phys. Lett.* **A24**, 2233 (2009), [arXiv:0901.2984 \[hep-th\]](#).
- [10] E. Manrique, M. Reuter, and F. Saueressig, *Annals Phys.* **326**, 463 (2011), [arXiv:1006.0099 \[hep-th\]](#).
- [11] D. Becker and M. Reuter, *Annals Phys.* **350**, 225 (2014), [arXiv:1404.4537 \[hep-th\]](#).
- [12] S. Nagy, J. Krizsan, and K. Sailer, *JHEP* **1207**, 102 (2012), [arXiv:1203.6564 \[hep-th\]](#).
- [13] D. Benedetti, *Europhys.Lett.* **102**, 20007 (2013), [arXiv:1301.4422 \[hep-th\]](#).
- [14] J. M. Pawłowski, (2003), [arXiv:hep-th/0310018 \[hep-th\]](#).
- [15] J. M. Pawłowski, *Annals Phys.* **322**, 2831 (2007), [arXiv:hep-th/0512261 \[hep-th\]](#).
- [16] S. Folkerts, D. F. Litim, and J. M. Pawłowski, *Phys.Lett.* **B709**, 234 (2012), [arXiv:1101.5552 \[hep-th\]](#).
- [17] C. S. Fischer and J. M. Pawłowski, *Phys. Rev.* **D80**, 025023 (2009), [arXiv:0903.2193 \[hep-th\]](#).
- [18] K. Falls, (2014), [arXiv:1408.0276 \[hep-th\]](#).